Meteoric Ionization : The Interpretation of Radar Trail Echoes

J. Baggaley

Abstract

An overview is presented of the developments during the key stages in the recognition of the mechanisms governing the behavior of meteoric ionization and an understanding of the radio-reflection processes. Meteors were the source that provided the enigmatic echoes: the fleeting radio returns seen in early ionospheric soundings, or as interference on communication links. The paper covers the key observations, probing techniques, and theoretical developments that enabled progress to be achieved in our understanding of the scattering processes from meteoric plasma, for the case of a reflection geometry giving rise to trail echoes. The development of meteor-echo theory enabled the realization of the value of radar meteors as valuable atmospheric and astronomical probes.

1. Introduction

The year 2008 marked the 80th anniversary of the first radio reports of strange fleeting echoes, which later became understood as plasma produced by the ablation of meteoroids. An originally enigmatic radio phenomenon, viewed on occasions as an interfering signal, became a valuable probing tool for the atmosphere. It enabled measurements of temperatures, scale heights, and wind-field, especially on micro-scales in a region difficult to access by other techniques. Radar meteors also became a tool for astronomy to gain a whole new perspective of monitoring Earth-impacting bodies. They advanced our understanding of the solar-system dust cloud. Radio techniques enabled us to measure the speed of meteoroids through the atmosphere and, using multiple sites, to determine their trajectories and orbits in space. For such programs, a foundation of the meteoric environment is required: the behavior of the created plasma, and a formulation of the mechanism of radiowave reflection. In the present work, the focus is on the class of meteor reflections now known as meteor-trail echoes, as distinct from the head echoes. Attempts to formulate radio scattering from the plasma produced by an ablating meteoroid could not be attempted until several controlling factors were known, such as a realistic appreciation of the geometry of and physical conditions in the created plasma. Experimentally, this was complicated in the 1930s by the confusion of what is now termed sporadic-E (E_s), with discrete reflections from the individual ionization trails of meteors in the height regime of 90-110 km. It is now recognized that an important agent in creating E_s is indeed the ionization deposited by meteors that is redistributed via charge exchange, and by the effects of wind-shear and geomagnetic field forces.

There were interpretation difficulties, because some early ionospheric-probing techniques employed swept-frequency modulation of CW or square pulses, with phase comparisons provided by reception from a distant transmitter and by measuring the interference between the direct ground signal and that reflected from the ionosphere. The frequency gradient provided the phase path and virtual sky-signal path. The technique made discrete targets difficult to identify, with multiple targets a problem in this method, resulting in interpretation difficulties in terms of identification of specific scattering entities. Reports described periods when a reflecting layer suddenly changed its virtual height, as seen on a (assumed) vertical sounding system (e.g., 1-6 MHz). Compared to early ionospheric studies, the very short durations of meteor returns were of quite a different time scale, making their recognition and study difficult.

In the early literature, the terms used for non-standard echoes from near 100 km included "abnormal E" and "intense E." Early soundings showed that sampling simultaneously from stations separated by ~100 km yielded largely unrelated echo structure. The horizontal and vertical structure of E_s clouds was only slowly understood.

By their very nature, meteors were detected as largely a byproduct of either propagation studies for early radio links, or by vertical radio probing of the ionosphere.

Jack Baggaley is with the Department of Physics and Astronomy, University of Canterbury, Private Bag 4800, Christchurch, New Zealand; Tel: +64 3 364-2558; e-mail: jack.baggaley@canterbury.ac.nz.

This is one of the invited *Reviews of Radio Science* from Commission G.

The advance of the ideas of meteor ionization and experimental methods provided an interesting development. In Section 2, it is useful to follow chronologically the events, noting some of the experimental arrangements.

2. The Period from 1920s to 1940: Observations and Speculations

In 1928, Heising [1], probing the *E* region with frequencies from 2.7 to 5.2 MHz, found sudden increases in nighttime ionization levels in place of the normal decrease that was known to occur after sunset. He included a rather picturesque description: "It would appear as though great masses of electrons are tossed into the atmosphere rather quickly...." He proposed a solar source of impacting electrons during the night as responsible. In 1929, Eckersley [2] studied propagation conditions monitoring arrival directions from stations transmitting in the range of 6 to 20 MHz, where penetration of the *E* region occurred, allowing reflection from the *F* layer. "Anomalous scattering into the skip zone" caused by ionized clouds below the normal *E* layer was noted. In 1930, Appleton [3] noted the variability of virtual height measured at 0.75 MHz, and remarked

> On such occasions, it seems as if there were some agency or agencies which either maintained the process of ionization....It appears as if on these occasions...there is some ionising agent present which can influence the dark side of the Earth.

In 1931, Skellett [4] made estimates of the ionization densities produced from individual meteoroid ablation, though with much over estimation because of the use of an unrealistic fraction of the meteoroid kinetic energy that is channeled into ionization, and also the exaggerated lateral extent of the plasma. Pickard [5] reported on studies of propagation conditions, carrying out several years of commercial forward scatter, which included correlations of increased nighttime signal strength with known meteor-shower activity.

In 1932, Appleton and Naismith [6] noted abnormal nighttime effects. Such studies took advantage of the spectacular meteor displays that deposit energy into the ionosphere. In the same year, Schafer and Goodall [7, 8] used pulse sounding, employing four spot frequencies between 1.6 and 6.4 MHz during known showers, especially the Leonids shower of 1931. They noted short-term nighttime signal changes. They suggested as candidates for such a source of ionization meteors producing what became termed "blanketing E_s" (although simultaneous magnetic activity related to a possible aurora complicated interpretation). Skellett [9], in pointing out that the inferred heights of radio features were similar to the heights of visible meteors, presented estimates of energetics to provide deposited ionization (the ionization probability used was too high by orders of magnitude, and the plasma train too large). The effect of the bulk influx of many meteors was also considered.

In 1933, Appleton and Naismith [10], operating a system in ionosonde mode and monitoring diurnally in a long series, "...recorded on a number of nights the ionisation in the lower region actually may increase....there is some agency which produces nocturnal ionization beyond the ordinary amount...." In 1934, Ratcliffe and White [11], using night-time probing on frequencies of 2 MHz and 4 MHz, noted "...nocturnal *E*-region...have a likely source of thunderstorms and magnetic activity...." Mitra et al. [12] used a swept-frequency technique to determine the

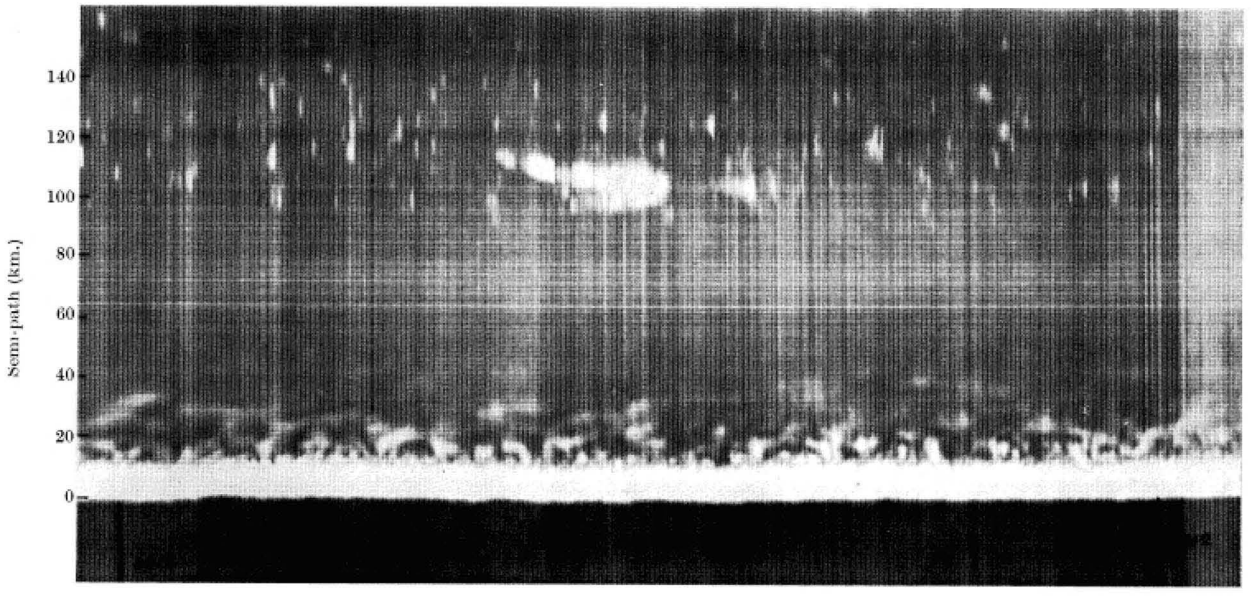

Figure 1. An echo-range time record at 6 MHz over a period of one hour [15]. The ordinate is range from 10 to 140 km. The 10 minute duration echo near the middle of the image is probably an E_s layer near the zenith. The other echoes from 100 to 140 km are meteors ([15] used with permission of the Royal Society of London).

Figure 2. An echo-range time record for a period of 40 s [17]. The ordinate range is from 0 to 600 km. All echoes are probably meteors, those with ranges out to ~380 km are at large zenith angles (reprinted by permission from Macmillan Publishers Ltd: Nature, [17], copyright 1937).

penetration frequency of the *E* layer, and measured high ionization densities coincident with the 1933 Leonids shower influx.

In 1935, Skellett [13] modeled likely meteor effects on the atmosphere, noting the self-luminous energy storage associated with enduring visible trains. He monitored transatlantic radiotelephone service over three years at shower times, measuring effects on propagation-fading disruption, with disruptions lasting seconds. He reported that effects were marked during the Leonid 1931 apparition. A separate 2.398 MHz sounding experiment was directed specifically for the Eta Aquarid shower period in July 1931, and also the Leonids in November 1931, using 2.398, 7.6, and 8.5 MHz sounding. Increases in ionization were attributed to individual overhead bright meteors, there being few such events during non-shower days. Attempts were made to estimate ionization densities and the effective electron-ion recombination coefficient.

In 1937, Appleton et al. [14], sampling at 6 MHz, noted "...*E*-layer bursts causes of abnormal *E* ionization ....we have also observed a peculiar type of reflexion at a height of 100 km which only lasts a few seconds....nocturnal abnormal *E* region reflexions is caused by the entry of ionizing particles into the atmosphere either in the form of bursts or in the form of a steady stream…charged solar particles or meteorites...."

The first time-sequence records seem to be those of Watson Watt et al. in 1937 [15], who, reporting vertical sounding at 6 MHz, presented filmstrip range-time displays clearly depicting meteor echoes lasting a few seconds (Figure 1 shows a one-hour record: their Figure 10). They stated that "...bursts of ionization at 105 km giving densities sufficient to return television waves at vertical incidence...persist for a fraction of a second."

Operating a swept-frequency 1-15 MHz sounder, in 1937 Bhar [16] reported on measuring the critical penetration frequency of the *E* region during the 1936 Leonid meteor shower. A close association was found, but no effect on the *F* region.

Also in 1937, Eckersley [17], monitoring a commercial station with a 9.127 MHz 40 kW 200 ms pulse with a 50 Hz pulse-repetition frequency (PRF), situated 19 km away from the receiver, used spaced-frame antennas and phase comparisons to deduce echo directions. This allowed the measurement of ground distance as well as virtual height. The author noted discrete "ionic clouds" present day and night, strongly suggesting meteors. A film range-time display of a 40-second time period is reproduced in Figure 2. In 1938, Skellett [18] supported the suggestion by Eckersly of a meteor origin, commenting on "...short-lived isolated clouds in which momentarily the ionization reaches a value much higher than normal."

In a 1938 scattering study, Pierce [19] monitored the signal strength from a 9.57 MHz 30 km-ground-distance station, noting signal bursts. Pierce appears to have been the first to be specific about the cylindrical geometry of the plasma (though he considered that critical reflection conditions operated, and that the plasma diameter was large compared with the probing wavelength, with the ionization density decreasing as the train expanded (under diffusion, although that mechanism was not stated). Scattering from such a "...long cylinder of ionization...under these conditions it is seen that no energy will be reflected to its source unless a perpendicular may be passed from the source to the path of the meteor." Interestingly, the author pleaded for simultaneous observations of visual meteors and the arrival angle of signal bursts.

In 1938, Appleton and Piddington [20] used a 8.8 MHz 3 kW 30 ms pulsed transmitter (Tx), radiating via a half-wave dipole $\lambda/4$ above ground, giving a broad vertical beam. They deduced the effective reflection coefficients on the basis of small ionization clouds and the virtual heights of transient echoes day and night, near 100 km. They noted, "There can be little doubt that these observations indicate the temporary existence of marked scattering centres in the

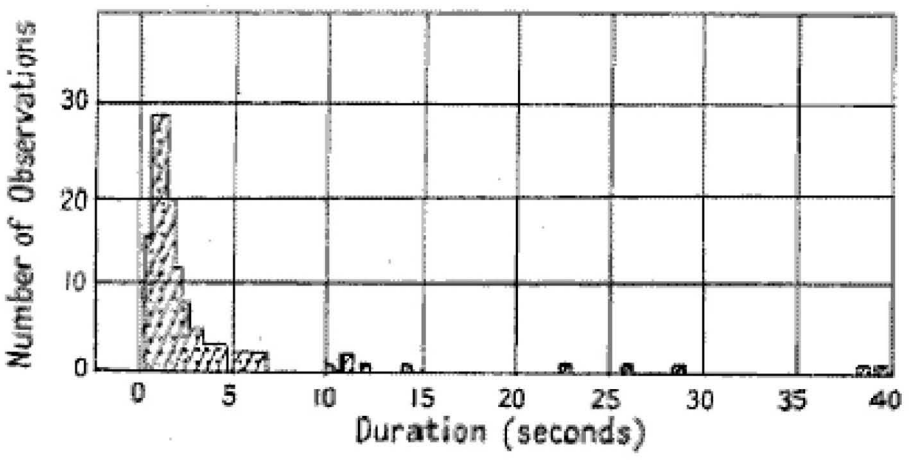

Figure 3. The duration distribution of meteor echoes at a frequency of 7.59 MHz [22].

ionosphere which form and disappear throughout the whole of the twenty four hours...due to some cosmic agency." Later, in 1939, Appleton et al. [21] described "intense-*E* being clouds of more intense ionization immersed in a simple region." They further stated that they "...noted a transient type of reflection lasting only a few seconds and caused by scattering from temporary ionic cloudlets, which is found by day and night round the 100 km level." They commented on the difficulties of recording such "fleeting echoes."

Concerned with effects on propagation, in 1940 Eckersley [22] studied scattering that occurred away from off-great-circle propagation paths using a 19.5 MHz transmitter with direction-finding antennas at a receiver (Rx) of 19 km separation. Recognizing the common occurrence of scattering processes, the author provided definitive short-term scattering characteristics of E_s and ion clouds (meteors). The first measurement of the duration distribution was provided with experimental evidence for many short durations (Figure 3, from Figure 11 of their paper), the form being instructive in providing clues about the reflection mechanisms.

The prevailing view expressed in work of the period speaks of "ionic clouds," "scatter clouds" – depicting a spherical assembly of electrons – consistent with the discrete echo of limited range spread that was commensurate with that expected from the radar pulse length. It is interesting that the idea of a column of ionization – analogous to the visible excitation trail of a meteor – only came later. It was not appreciated that a narrow column of electrons of length similar to visible trails would in fact produce an echo of discrete range (see Section 4.3). In addition, the geometry of the reflection process results in reduced sensitivity to meteors near the zenith, so that vertical probing was in fact the most disadvantageous antenna-pointing direction (see Section 4.3).

In 1941, Blackett and Lovell [23] examined the possible production of an ionization column resulting from proton impact produced by primary cosmic rays. The origin of the "scatter echoes" was confirmed later as not being from cosmic rays. However, the geometry and radar scattering mechanism was established by this paper: "A cosmic ray shower of high energy produces a long narrow cylinder of ionization traversing the whole atmosphere." They established the essential geometry of the reflection process: the shape of the target means they employed a scattering length of one Fresnel zone (see Section 4.3). It is of interest to note that the paper was composed (August 1940) at a radar station that was often under attack from aircraft [24].

The association of visual meteors with reflections at 3 MHz and 6.4 MHz was studied by Pierce in 1941 [25], to confirm the governing geometry: "...energy of impact sufficient to ionize any particle with which it comes in contact. Thus a line of ionized atoms or molecules is established along which the density of free electrons is very great. The charged particles immediately begin to diffuse radially...." The author made an estimate of the electron density from the echo duration. However, an incorrect reflection coefficient was employed: an extended ionization column was recognized, but the column diameter was incorrectly assessed as being much greater than the operating wavelength (implying diameters > 100 m).

3. The Period 1940 to ~1952: Interpretations

The period of 1939-45 provided an impetus for three reasons:

1. Equipment: a large number of radar tracking stations employing high pulse power with narrow-beam steerable antennas directed to low elevation (rather than sampling towards the zenith), to provide aircraft detection and tracking, became available;

2. Personnel with defense experience and subsequent availability of equipment (and in some cases military personnel to assist). Similar equipment served to advance the early work in radio astronomy.

3. The parallel development of theoretical work to understand the types of observed echoes.

3.1 Radar Equipment and Techniques

Many of the radars that were produced during WWII formed an interesting subject in themselves. Some were ideal for the task of providing foundation observations for theoretical formulations of reflection coefficients, echo behavior, and tools for both atmospheric and astronomical studies. Especially suitable for the purpose were the mobile gun-laying (GL) radars, developed in the UK circa 1940, operating at 72 MHz and attached to antiaircraft units. The GL2 unit was capable of a power output of 150 kW of 3 ms pulses at 1 to 2.2 kHz pulse-repetition frequency with a 25 kV dc supply. This was achieved from a pair of cathode-driven VT98 triode (also labeled type CV1098) power tubes using forced-air cooling. The tube (Figure 4) was developed from the previous VT58 in order to secure greater emission under pulse conditions by incorporating filaments using thoriated tungsten. The GL2 employed a system of dipole antennas at differing heights and horizontal separations for elevation and azimuth fixing. With minor modifications, this equipment proved ideally suited as a meteor-research tool. Other systems, such as the Chain Home (CH) system, used a frequency (20-30 MHz) that was actually more sensitive for meteors (see Section 4.4).

Figure 4. The transmitting tube, type VT98.

They used water-cooled transmitter tubes, required large metal antenna supporting masts in operational service, and required a team of personnel to operate.

There were associated advances in techniques that enabled efficient operations and that proved valuable for meteor use. These included the provision of a common antenna for both transmitting and receiving (the transmitting/receiving switch employed $\lambda/4$ stubs and spark gaps), and the development of polythene as improved insulating material for coaxial cables used in transmission lines and impedance-matching sections. The introduction of the Chain Home Low (CHL), Ground Controlled Interception (GCI), and similar radars operating at 200 MHz and the later magnetron-powered radars at 10 cm (for improved image resolution), were not as useful. Meteor scattering is a long-wavelength phenomenon (see Section 4.4): during the 1960s, the author built and operated a radar system for meteor research operating at 17 MHz, which was constructed in part of surplus military components.

Many GL2 units were produced and some rendered meteor service around the world. One unit was used up to 1975 by the author at the University of Canterbury's station near Christchurch in New Zealand. The author also visited a unit used at the Englehart Observatory near Kazan, which operated until about 1985. It was the eventual lack of a supply of VT98 tubes that caused the end of the GL2's use for these two radar-meteor programs.

3.2 Experimental Work

During the operation of defense radars in the UK, echoes were commonly observed on Chain Home and gun-laying units (termed "scatter clouds" or "short duration

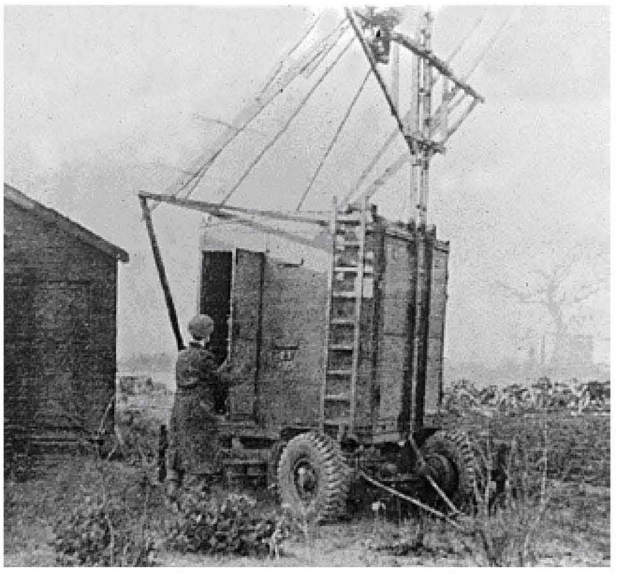

Figure 5. The first mobile ex-army GL2 radar used from 1945 for meteor studies at Jodrell Bank, near Manchester, UK (photo provided by the University of Manchester).

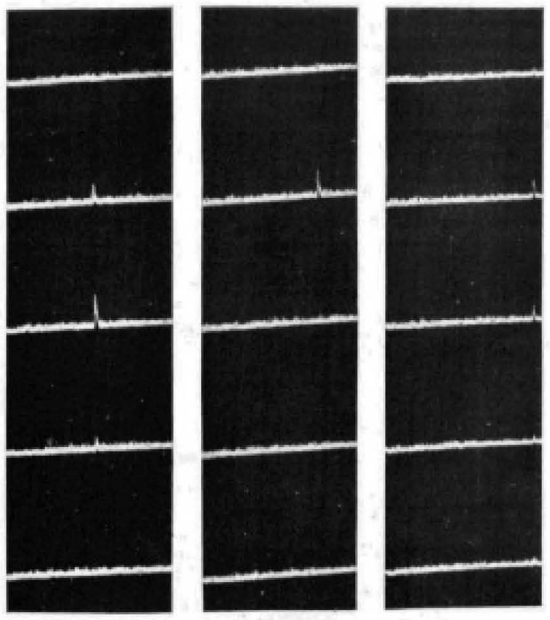

Figure 6. A sequence of echoes recorded on film at 16 frames per second. The range interval shown is 80 to 125 km ([30], IOP Publishing Ltd., used with permission).

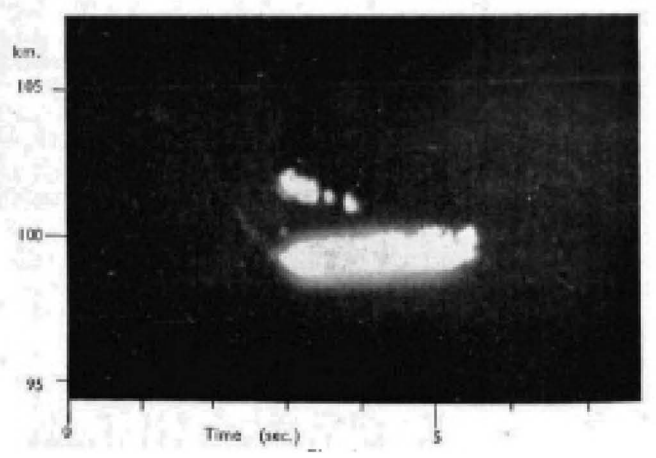

Figure 7. A range-time radar 55 MHz 8 s sequence [30]. The echo at range 102 km was composed of several features (probably) caused by atmospheric turbulence. The echo at range 100 km had a body (transverse geometry) echo, showing a drift in range caused by a radial wind and a faint head echo lasting 0.5 s with a hyperbolic range-time characteristic, from which the meteor speed can be derived. That speed would be a lower limit, since the aspect angle between the trajectory and the radar beam line of sight was not known ([30], IOP Publishing Ltd., used with permission).

scatter echoes") at frequencies well above the critical frequencies for either normal or abnormal (E_s) layers, where such echoes often interfered with aircraft detection and tracking. The availability of mobile radar units and photographic recording led to an intense period of observational work during 1945-48. This led to rapid progress where the need was recognized to modify the antenna-elevation response for optimum meteor detection. For example, the work at Jodrell Bank, near Manchester UK, starting in late 1945 employed a modified GL2 system (Figure 5), with the later addition of an army searchlight mounting for an array of fully steerable Yagi antennas, enabling full-sky surveillance.

In 1945, Eckersley and Farmer [26], using a frequency of 7.6 MHz, measured the direction of arrival and polarization state of echoes near 100 km for both E_s and individual meteors. They noted rapid polarization changes. They considered that such echoes were incompatible with a meteor source, because their phase behavior suggested rapid changes in arrival direction due to suggested multiple paths (but see Section 4.4 for theoretical phase behavior). It was noted that meteors reflected at frequencies well in excess of the critical frequency of the *F* region: 45 MHz TV (Appleton [27]) and at 105 MHz (Ferrell [28], using a US military SCR270B radar unit).

In 1946, Hey and Stewart [29] carried out a surveillance from October 1944. They recognized that "columns of ionized gas....present their echoing areas when viewed at right angles to their length." Operating ex-military 150 kW radars from 42 to 75 MHz, equipped with Yagis, they recorded the Lyrids meteor shower (April 20, 21, 22, 1946), while maintaining a visual watch for overhead meteors. They so confirmed the association of echo activity with showers. In addition, recognizing the importance of the reflection geometry, they were able to deduce the radiants (upstream meteoroid direction) of a stream (not for individual meteors: the technique requires several members) by employing the different radar-system responses governed by the meteor-reflection orthogonal geometry due to different antenna-pointing directions. They thus for the first time identified daytime meteor streams.

Extending their earlier work, in 1947 Hey and Stewart [30] presented a time sequence (cine film, 16 frames per second) aimed at quantifying the rapid decay times of echoes (Figure 6). From this, they made the significant finding that many echoes (at 73 MHz) had decay times of the order of 0.06 s. Using multiple radar stations, they measured echo-height distributions. With the important recognition of the controlling geometry, they deduced radiant coordinates for the Delta Aquarid meteor shower of July 29, 1946, and the Giacobinids (that spectacular event providing a focus of many observational projects and impetus to our understanding) on October 10, 1946. They also reported much reduced echo rates, using sampling at the higher frequency of 212 MHz. In a key observation, they were the first to report the head echo shown in Figure 7. This is the reflection from the plasma surrounding the meteoroid itself – weak compared with the broadside echo – with the range-time hyperbola function providing an estimate of the meteoroid's linear speed in the atmosphere. In 1947, Prentice et al. [31] mapped the Giacobinids and other streams. By orienting the directive Yagi array in a different direction with respect to the shower radiant, they were able to confirm the scattering geometry in a dramatic way during the Giacobinids display. The optimum reflection

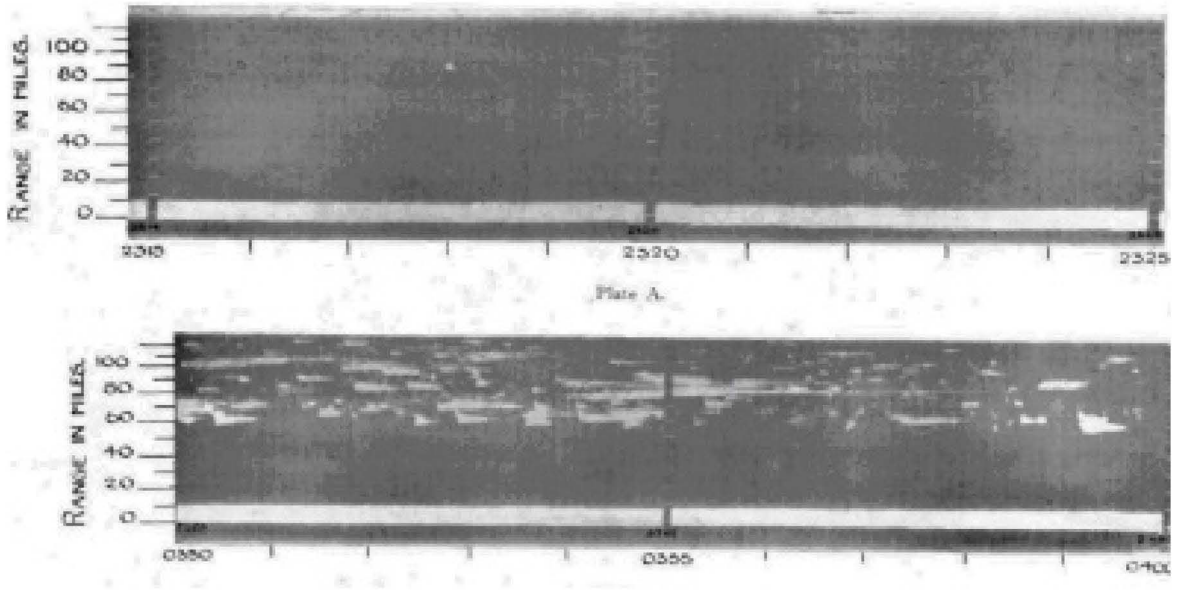

Figure 8. Echo range-time records at 27 MHz with 10 minute records: (upper) October 9, 1946, GMT 2315; (lower) October 10, 0350 at time of the Giacobinid shower influx (reprinted by permission from Macmillan Publishers Ltd: Nature, [33], copyright 1946).

geometry was also used to deduce shower radiants by McKinley and Millman in 1949 [32].

As reported in 1946 and 1947, Appleton and Naismith [33, 34] also used film recording of a CRT display. Operating at 27 MHz with 15 ms, 50 Hz pulse-repetition-frequency pulses directed vertically, they maintained a two-year survey daily from January 1944. This included the Giacobinid shower of October 10, 1946. Figure 8 shows their range-time plot, in which Plate B showed the very high influx rate from October 10, 0350 to 0400 GMT. The Giacobinids were also monitored using 3 MHz by Pierce, reported in 1947 [35], recording a meteoric *E* layer with substantial deposition sufficient to maintain ionization in the layer for four hours.

In 1947, Eckersley [36] proposed an analogy of meteor reflection with the case of alpha-particle scattering from heavy atoms. This comparison is not applicable, since the geometry is quite different because the model was of a small spherical-like cloud, but the meteor case is not spherically symmetrical. It was also mistakenly proposed that the ionization target should move with the meteoroid (as is actually the situation for the quite different case of the head-echo-producing plasma).

In 1948, Eastwood and Mercer [37] reported on a surveillance from January 1945 to July 1946 at 20-45 MHz, with a vertical stack of horizontal half-wave dipoles and cine-camera photographic CRT display. This was able to record echo amplitude as a function of time for individual echoes at a sampling rate of 25 Hz. Diurnal, seasonal, and solar-cycle rates were studied, as well as the dependence of the echo range distribution on elevation pattern, and its relation to antenna type and ground height. Examination was also made of the echo rate dependence on operating radar frequency, and a study of the influence of the July 9, 1945, solar eclipse.

In 1948, Allen [38] described forward scatter at 40 MHz (carried out during 1943), reporting chart recording of "bursts," and noting that longer scatter durations occurred at 10 MHz. Diurnal and seasonal forward-scatter bursts from several commercial stations were examined. The study noted simultaneous visual meteors and bursts via scatter to indicate that reflections were orthogonal to the trajectory. The forward-scatter configuration was analyzed by Geometrical Optics with modifications by Manning and Villard in 1948 [39].

The diurnal-seasonal rate characteristics mapped [37, 37, 38] can be interpreted in terms of astronomical effects. Although influenced by the orientation and width of the radar antenna's radiation pattern, the meteor influx at any latitude is dominated by the elevation of the Earth's apex (the upstream vector of the Earth's orbital motion) above the radar's local horizon.

A summary of the theoretical understanding of the meteor-scatter process to date was provided by Lovell and Clegg in 1948 [40]. They presented a model of the formation process of the plasma trail with correct geometry, and also measured the wavelength dependence of meteor-reflection coefficients. This work was later extended by Kaiser and Closs in 1952 [41].

4. Meteor-Scattering Theory

A firm theoretical foundation of radiowave scattering from meteoric ionization is necessary to provide sound linkages between the interaction of meteoroid bodies with the atmosphere and the relationship between the characteristics of returned signals and other parameters. These parameters include meteoroid mass, trajectory, speed, and conditions in the meteoric plasma and its complex meteor environment: atmospheric parameters, wind field, and geomagnetic field.

There are two particular radar-observing geometries for meteor scatter that have evolved (originally, from distinctly observed echo types). The first is reflection orthogonally from the linear column of ionization, so that scattering takes place from a long (~1km) cylinder of plasma, observed employing a transverse geometry producing a trail echo or *body echo*. The second is reflection from the spheroidal plasma immediately surrounding the ablating meteoroid, observed employing radial geometry: the *head echo*. In the former configuration, the radar's line-of-sight is strictly orthogonal to the meteor trajectory, and in the latter, the line-of-sight is broadly radial. Here, we follow the above early observational work of Sections 2 and 3, and focus on the transverse echo situation. Some aspects of the head echo (see Section 4.4) have been described [42], and some associated studies have been recently outlined in the *Radio Science Bulletin* [43] and by Mathews [53].

The formulation of a theory of radar scattering for the transverse reflection geometry, producing a broadside body echo, can be regarded in essentially two stages:

1. To treat the ionization column as an instantaneously formed long column, which expands by ambipolar diffusion, retaining a Gaussian cross section (ignoring any distortion from geomagnetic field forces), and remaining stationary (not moving with the neutral atmosphere). It is thus an assembly of electrons of time-increasing radius.

2. To superimpose a modulation produced by the finite creation time of the plasma.

4.1 The Scattering Cross Section

For an assembly of electrons in the meteor case with electrons at essentially the same range, the effective total scattering cross section depends on the summation of phase contributions from individual electrons, on the overall geometry, and on whether secondary radiative effects are present (depending therefore on electron number density). At meteoric altitudes (~100 km), electron-neutral collisions can be neglected in the radiowave scattering process. Coherent reflection from the meteor plasma provides the radar target. A single electron has a scattering cross section to an incident electric field of $\sigma_e = 4\pi r_e^2 \sin^2 \gamma$, where r_e is the classical scattering radius, and γ is the angle between the *E*-field vector of the incident wave and the scattering direction. For the radar backscatter case, with co-located transmitter and receiver, $\gamma = 90°$ and $\sigma_e \sim 10^{-28}$ m^2.

The signal power available to a receiving antenna, p_r, from a target of scattering cross section σ at range *R*, using transmitting and receiving antennas of gains G_T and G_r, with transmitting power P_T and operating wavelength λ, is of the standard form

$$p_r = \frac{P_T G_T G_r \lambda^2}{64\pi^3 R^4} \sigma \,.$$

The problem reduces to determining an expression for the total scattering cross section, σ, for the particular equipment, geometry, and meteor train parameters.

4.2 Behavior in Limiting Cases

The large range of masses of meteoroids incident on the Earth's atmosphere means a substantial range in ionization densities is generated. The ionization distribution has the form of a tapered cylinder, with a larger radius at greater heights resulting from the larger atmospheric mean free path and the finite time to diffuse. For the limiting case of a weak plasma, the radio waves pass through the plasma unaffected. The scattering of the incident radio waves from electrons takes place independently without any secondary or interference effects. The total scattering is then the summation over all electrons in a cross section of the meteor train. Such a situation is described as an *under-dense* train. At the instant of formation of such a train, if the plasma radius at formation, r_0, is very small compared to the radar wavelength, λ, then for evaluating the reflection, all electrons can be considered to be situated on the train's axis and with the same scattering phase. For the opposite case of an extremely dense plasma, secondary scattering is an important feature, and the incident wave is grossly disturbed. The dielectric constant of the medium is sufficiently negative for total reflection to occur at some critical boundary. Thus, as diffusion increases the dimensions of the boundary, the reflection coefficient increases. Train expansion reduces the electron number density on the axis so the dielectric constant becomes less negative, the critical radius collapses to the train axis, and subsequently, individual electron scattering operates as the incident wave penetrates the plasma column. Such a dense expanding train can be regarded in its reflection behavior for the limiting high-electron-density case as a metallic cylinder the radius of which expands for a period before collapsing. This regime is termed an *over-dense* train.

The transition between the two regimes can be defined in terms of the attenuation of the incident wave. Since the dielectric constant of the plasma is negative for the over-

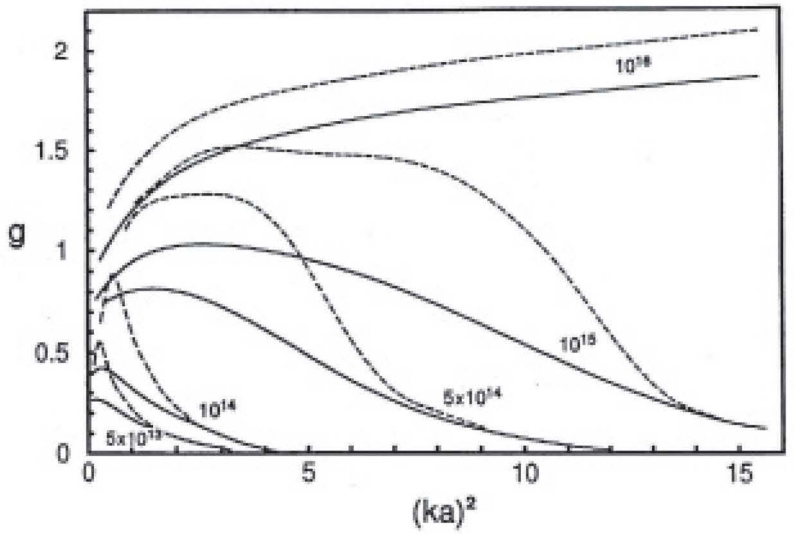

Figure 9. The reflection coefficient as a function of time: full line: parallel polarization; broken line: transverse polarization (reprinted from [44] with permission from Elsevier).

dense case, the incident wave is an evanescent wave. If the plasma is of such a critical density that the amplitude of the evanescent wave is reduced to e^{-1} on the axis (in analogy with the skin depth for a metal, although for a metal, the concept employs the ohmic conductivity), the train plasma is described as being transitional. This definition means that the attenuation distance, equal to the radius of the cylinder, a, is $\lambda/2\pi$. The corresponding critical electron density, $n_c = q/\pi a^2$, can be related to the radiowave frequency and plasma conditions by $n_c = \omega^2 m\varepsilon_0/e^2$ with m and e being the electron mass and charge, respectively, and ε_0 being the free-space permittivity. The corresponding critical electron line density is $q = 8.9\times10^{13}$ m^{-1} (a value that is independent of the probing radio frequency). This was derived assuming a cylinder of uniform cross section (a more-realistic Gaussian profile changes the value only slightly). Such a value corresponds to a meteor optical magnitude of approximately +5 (near the limit of unaided-eye visibility).

4.3 Reflection from an Instantaneously Formed Column

The time variation of the reflection coefficient cannot be derived in analytical form. A full-wave treatment, employing numerical solutions, is necessary [44]. To keep the problem tractable, it is assumed that (ambipolar) diffusion operates, retaining a Gaussian cross section with initial size established by thermal expansion to a few mean free paths. A more complete treatment shows that the distortion caused by the geomagnetic field can have a marked effect when at large heights the electron-neutral collision frequency becomes small compared with the electron gyro-frequency. Including fully the polarization field within the meteor plasma and the effects of ambient background ionization provide a more detailed analysis (e.g., [45]).

In the general case, the interaction of the EM wave is considered in terms of a reduced dielectric constant within the plasma. A plane wave incident at arbitrary angle to the column's axis can be resolved into components parallel to and transverse to the axis. Within the column, the E and B fields must satisfy Maxwell's equations, and we expand the field components in cylindrical harmonics. Outside the train, the field is the sum of the incident plane wave and the scattered (cylindrical) wave. The incident waves are expressed in terms of a series of Bessel functions. The cylindrical wave is expressed in terms of Hankel functions of the first kind, the order of which is dictated by the geometry and radial dependence for this case. To yield reflection coefficients, numerical solutions of the equations are matched onto asymptotic forms representing the incident and scattered waves: the field components at the matching radius. Numerical integration of the field equations [44] provides solutions (powerful computing techniques that have become available allowing such full-wave solutions were not available to aid early attempts [41]). These present reflection coefficients and map polarization changes in the scattered field early in the echo lifetime, and the resonance that can occur when the incident electric vector is transverse to the train's axis (so the electrons are being driven across a density gradient, producing charge separation).

Solutions are presented in terms of time from train formation at $t = 0$. q is the electron linear density, in electrons m^{-1}, under a diffusion coefficient, D, where the e^{-1} plasma-column radius, a, is given by $a^2 = r_0^2 + 4Dt$, with r_0 being the initial Gaussian radius. Some results of such a full-wave treatment, providing the complex reflection coefficient, are shown in Figures 9 and 10, where the orthogonal plane polarizations are shown. The reflection coefficient, g, is related to the scattering cross section by $g^2 = \sigma\pi/2R\lambda$. λ is the operating free-space wavelength, and the wavenumber is $k = \lambda/2\pi$. For $ka > 1$, the horizontal axis in Figure 9 is then approximately proportional to time. Figure 9 shows the reflection coefficient, g, for the parallel and transverse cases as a function of q over a range of line densities showing the echo-transition region, where the change from strictly exponential decay for small q can be

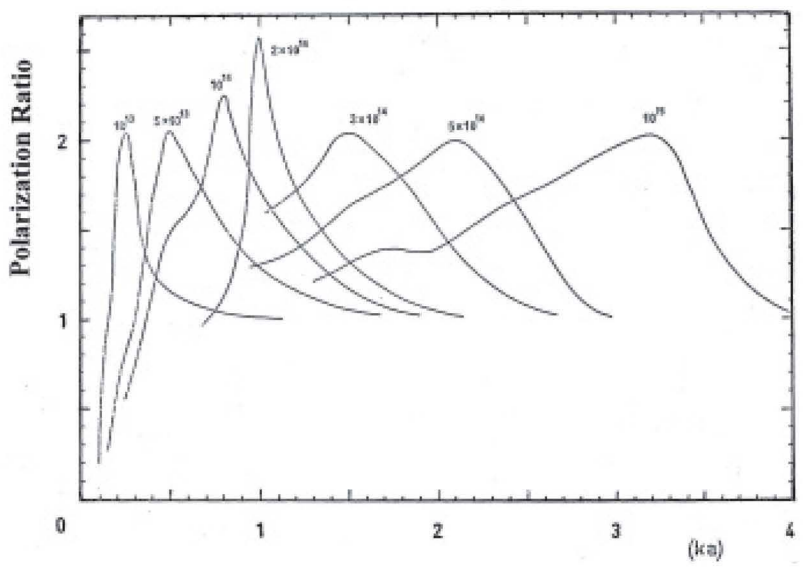

Figure 10. The time variation of the polarization ratio for various q electrons m^{-1} (reprinted from [44] with permission from Elsevier).

seen. It is clear that there is a range of a factor of $\sim 10^2$ in q in the bridging region between the two limiting cases. Figure 10 shows the polarization ratio and the resonance peak for the optimum value of *ka*. Two situations might be envisaged. If the train is created with a small r_0, then it has to diffuse to a critical radius for resonance to occur. If r_0 is too large, then no resonance condition will be possible.

The echo behavior can be summarized as follows.

4.3.1 Under-Dense Echoes

The later stages of an under-dense echo are dictated by diffusion. As the plasma expands, phase summation of the individual electron contributions in a train's cross section results in a reduction in the echo reflection coefficient, *g*. If a Gaussian train cross section is maintained during expansion, the change in *g* will be an exponential function of time. The echo decay is described by $\exp(-t/t_d)$, with $t_d = \lambda^2/32\pi^2 D$. The role of the geomagnetic field in producing anisotropic diffusion has been emphasized. The resulting distortion of the plasma column produces a look-angle dependency on the decay of the radar echo. For simplicity of treatment, assuming a Gaussian profile and circular symmetry at formation, the plasma column distorts into a generally elliptical cross section. With inhibited diffusion, the echo decay rate can be very much less, and enhanced echo lifetimes can result under certain geometries.

4.3.2 Over-Dense Echoes

A full treatment of the reflection from a Gaussian dense plasma is complex, because of the effects of the weaker ionization in the outer regions of the column on the wave. However, a simple picture enables an estimate to be made of the echo characteristics of an over-dense plasma.

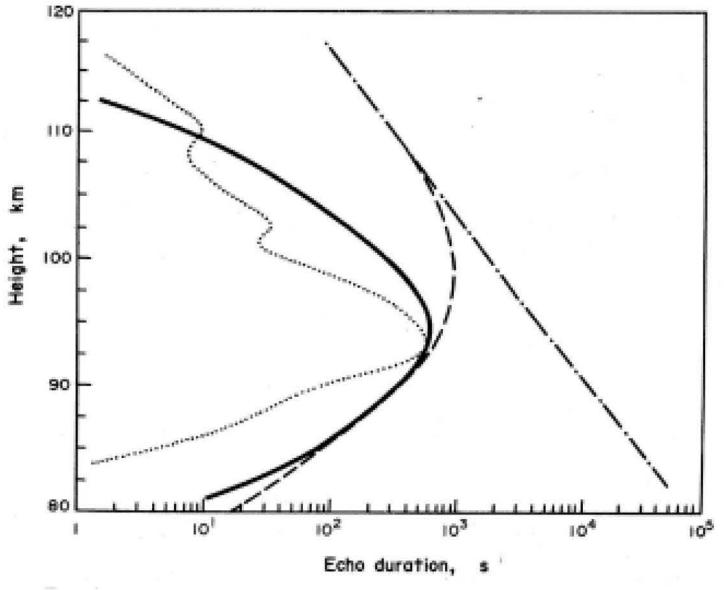

Figure 11. The height variation of over-dense meteor echo durations for a radar frequency of 30 MHz (reprinted from [47] with permission from Elsevier)
–●–●–●– : the expression $T_{ov}q = 6\times10^{18}\ m^{-1}$ all heights.
- - - -: the expression T_{ov} and including ionic reactions, $q = 6\times10^{18}\ m^{-1}$ all heights; ——— *: the expression T_{ov} including ionic reactions height profile of deposited ionization with $q_{max} = 6\times10^{18}\ m^{-1}$ at 88 km. :* ●●●●●●● *measured for enduring Perseid echo [46].*

For a general over-dense plasma, there will be a critical radius, r_c, at which the plasma has a critical electron number density, n_c (for which the dielectric constant is negative). This will occur when

$$n_c(r_c,t)=\left(\frac{q}{\pi a^2}\right)\exp\left(-\frac{r_c^2}{a^2}\right).$$

Defining the duration of an over-dense echo as the time for the axial electron number density to fall to n_c, so that $n_c(0,t)=q/\pi a^2=\omega^2 m\varepsilon_0/e^2$, then the over-dense duration is

$$T_{ov}=\left(\frac{e^2}{4\pi\varepsilon_0}\right)\left(\frac{q}{\omega^2 D}\right)-\left(\frac{r_0^2}{4D}\right),$$

where the last term represents the "age" of the train at the start (the time to diffuse to a radius of r_0) under normal diffusion, and is only comparable with the first term in the upper meteoric region, >105 km. This diffusion-limited echo duration will be modified by the action of ionic processes removing electrons from the train plasma. Models can be made of how echo durations will be curtailed by the effective decrease in the value of the line density, q (chemistry influence is usually negligible for under-dense echoes). Ozone is expected to be the dominant gas initiating the chain of reactions responsible for the deionization of trains. Because of the solar control of lower thermosphere O_3 densities, the durations of echoes under daytime conditions will therefore be markedly reduced compared with nighttime. The modeled electron-loss characteristics can then be inserted in the echo durations to model the echo lifetimes as a function of altitude. Illustrations are given (for a radar frequency of 30 MHz) in Figure 11 of how T_{ov} values are expected to vary with altitude. The approximately exponential downwards increase in T_{ov} due to both an increase in q (for a given meteor) and an atmospheric-density increase are countered by the increasingly short chemical lifetime of electrons below ~95 km. This relates to the observation of occasional long-enduring echoes (for example, [20, 22]). A specific illustration of the effect is to be found in the altitude variations of long-enduring Perseid meteor echoes [46]. In that study, triple-station ranging fixed the echo altitude, so that the echo duration could be followed by the radar system as a function of altitude during the persisting ~ 9 min train. As predicted ([47]), the most enduring section of the diffusing plasma occurred at an altitude close to 93 km (Figure 11).

This sensitivity of echo behavior to ambient gases presents a method of monitoring the atmosphere. Measurements of the characteristics of radar-echo lifetimes can enable estimates to be made of the altitude profiles of the important atmospheric species O_3 ([48, 49]) in a altitude regime that is largely inaccessible by other techniques.

It is instructive to provide an example of echo-duration characteristics by reference to a historical case. The first reported echo-duration distribution measurements [22] can be interpreted in terms of the theoretical behavior. In Figure 3 of this work, there was a preponderance of short echoes, with 85% having a duration < 2.5 s and 6% > 10 s. The types of radar systems employed in the period, ~1940, using a transmitting power of a few kW and low antenna gains, would have had a limiting sensitivity of $q \sim 10^{12}\,\mathrm{m}^{-1}$ This corresponds to a meteoroid mass of $\sim 10^{-6}$ kg, and a visual magnitude of ~+10. The meteoroid population mass content follows a power law: there are many more small bodies than large bodies. As a consequence, the radars of this type detect many more under-dense short echoes than over-dense. The mode duration [22] was ~ 1.5 s, and from the expression for t_d above and an operating frequency of 7.59 MHz, the inferred diffusion coefficient, D, was 6.6 $\mathrm{m^2 s^{-1}}$, corresponding to a height of ~95 km [50]. This is a representative average ablation height for meteors.

More recent work has extended the treatment to recognize the role of plasma instabilities produced by ionization gradients and E fields created by the action of ambient neutral wind, or resulting from the action of diffusion across the geomagnetic field [51]. The growth of instabilities depends on the background general ionospheric ionization. Such plasma instabilities result in meter-scale irregularities, having a geometry controlled by the geomagnetic field, which may result in range-spread echoes and enhanced echo durations. The effect depends on the angle between the radar-echo direction and the meteor trail [52, 53, 54].

In the interaction of an ablating meteoroid with the atmosphere, the ionization along the trajectory is distributed so that the electrons and ions are deposited over the physical path length. This is governed by the mass-loss rate, which depends on the track's zenith angle, Z, so that $q \sim \cos Z$. An echo close to the zenith would be generated by a meteor with a near-horizontal trajectory and therefore a low q, and, in consequence, low detection rates. This bias would be responsible for the sparse meteors recorded for vertical ionospheric-sounding antennas in the 1930s, and for improved detection conditions using low-elevation aircraft-seeking radars in use from 1940 to 1945.

In the case where the transmitter and receiver have a substantial ground separation, the situation is that of forward scatter (γ not equal to 90°). The geometry becomes that of oblique reflection, being an extension [55] to the method outlined here.

4.4 Reflection from the Developing Plasma

In order to complete the modeling of the time variation of meteor scattering, it is necessary to modulate the instantaneously formed ionization train by taking into account the finite time interval to create the plasma column.

This formation process is modeled by assuming that the free electrons can be regarded as essentially confined to the axis (so $r_0 \sim \lambda$). This approach permits an analysis in terms of diffraction, where the relative phases of contributions of segments of the forming plasma sum to provide the scattered field. The time behavior of the body echo arises as the meteoroid deposits ionization over increments in length at a changing range, and therefore with changing phase. The concept of a Fresnel "zone" (rather than "interval"), often used in describing meteor diffraction, arises from its use in the two-dimensional case in optical diffraction on a plane surface, and derives from its use in describing the operation of the zone-plate optical device. Such a zone plate is described by annuli having successive (usually π) increments in phase. Such a geometry, employing a zone or area, is not strictly appropriate in the present meteor case, where the contributions are distributed in one dimension. The term "Fresnel interval" or "Fresnel length" is more realistic in the meteor case involving linear scatter, producing a cylindrical wavefront.

The time variation of the scattered electric field and its phase – the complex electric field – is the vector sum from elements along the meteoroid's trajectory, with contributions from adjacent Fresnel intervals being π out of phase. The oscillatory electric field provides the backscattered echo, with the received power at the antenna being

$$p_r = \frac{P_T G_T G_r \lambda^3 \sigma_e}{256\pi^3 R^3}\left(C^2 + S^2\right)q^2,$$

where C and S are the Fresnel integrals. These are defined by

$$C = \int_{-\infty}^{X} \cos\left(\frac{\pi x^2}{2}\right)dx$$

and

$$S = \int_{-\infty}^{X} \sin\left(\frac{\pi x^2}{2}\right)dx.$$

X is the Fresnel parameter, proportional to the distance Vt (with V being the meteor velocity) of the scattering element from the origin ($X = 0$), measured in Fresnel intervals: $X = 2Vt/(R\lambda)^{1/2}$. The maximum value of the resultant electric field can be regarded as due to an effective train scattering length of about one Fresnel interval, $\sim (R_0\lambda/2)^{1/2}$, either side of the $X = 0$ condition (the t_0 point where the trajectory is orthogonal to the radar sight line). The resultant maximum scattering cross section depends on the square of the number of contributing electrons. The maximum echo power available at the radar antenna occurs when the Fresnel parameter $X = 1.217$. Thus,

$$p_r = 1.26\times10^{-32} P_T G_T G_r (\lambda/R)^3 \left(C^2 + S^2\right)q^2$$

watts, with q electrons m^{-1}.

The time behavior of the received signal has a close optical analogy with the angular changes in light intensity in the case of diffraction at a straightedge in classical optics, or the cylindrical-wavefront radio electric field in the radio shadow produced by an obstacle. The complex diffraction

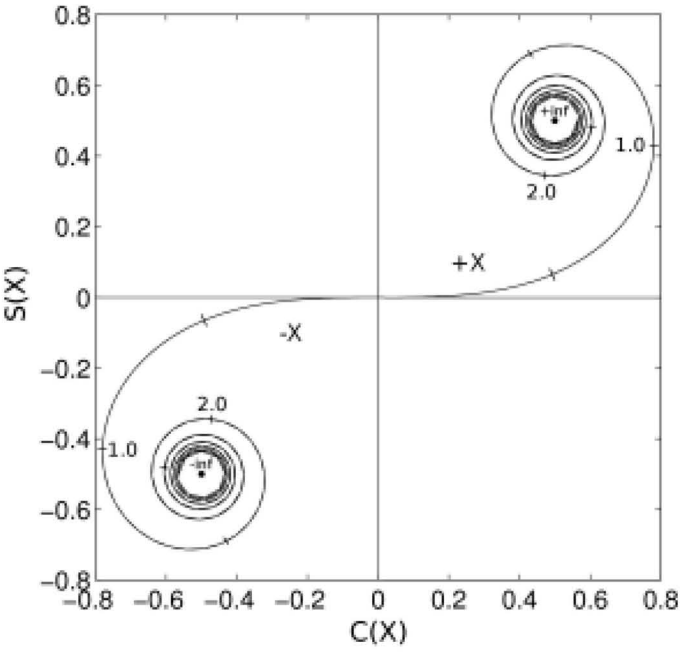

Figure 12. The Cornu Spiral: an orthogonal plot of $C(X)$ and $S(X)$. The distance along the meteor trajectory from the orthogonal point on the meteor trajectory is represented by the distance along the curve from the (0,0) point to the limits of ± 8.

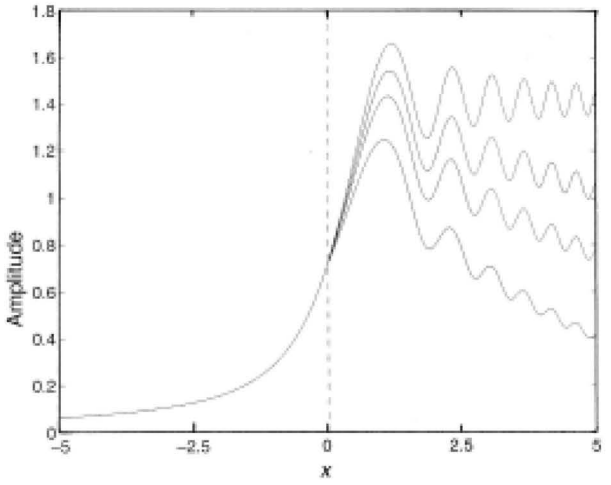

Figure 13. The time variation of the scattered electric field (echo amplitude in arbitrary units) with X as the Fresnel parameter proportional to time. The top trace is for no diffusion; the three other traces show the pattern of echo decay for cases of increasing diffusion.

behaves in these cases in a way described very usefully by the Cornu spiral (Figure 12). The relative echo amplitude at any time (and therefore the value of X) is given by the length of a vector from the point $C = -0.5$, $S = -0.5$, ($X = -\infty$), to a point having a particular value of X on the curve. The time variation of the echo-diffraction electric field is proportional to $\left(C^2 + S^2\right)^{1/2}$ (Figure 13). The variation of phase, ϕ, is described (Figure 14) by $\tan\phi = -(0.5+S)/(0.5+C)$. As the meteor approaches the orthogonal position t_0, there is a rapid rise of the signal as an increasing number of half-period Fresnel intervals contribute. The phase increases monotonically (as the meteoroid-generated plasma approaches the radar), reaching a maximum of $-\pi/6$ (strictly, $-29.4°$) when $X = 0.57$ (defining the phase as $-\pi/4$ when $X = 0$).

As the meteoroid moves through successive Fresnel intervals, both the signal and its phase oscillate. At the instant of maximum ($X = 1.22$), about 90% of the energy is contributed by the central Fresnel interval, extending over a distance along the meteor ionization train of about 2 km for an ~30 MHz radar. Both the post-t_0 oscillatory echo amplitude [56] and the pre-t_0 phase gradient [57, 58] provide techniques for measuring the meteor's scalar speed. The early life of a meteor echo formed with orthogonal geometry is dictated by diffraction, independent of the q value and of whether an under- or over-dense plasma. Indeed, the rise time of an echo can yield an estimate of the meteoroid's speed [59]. After the t_0 point, the phase, while undergoing small ($< \pi/20$) oscillations, may show gross phase changes caused by the motion of the plasma in the ambient neutral wind. This provides a technique used to monitor the atmospheric wind field in studies over a wide range of scales, from gravity waves to planetary waves. All of these phase effects would have contributed to the rapid phase behavior noted in early [26] reports.

For the case of the head echo (for example, Figure 7) produced in the radial-reflection geometry, a similar analysis can be applied to make an estimate of the scattering. We will not discuss that geometry further here, except to note the expected difference in scattering cross sections. Since when viewing the head plasma with radial geometry the Fresnel size is $\sim \lambda/4$, the ratio of the radial to transverse scattering cross sections is $\sim \lambda/8\pi^2 R$, or approximately 10^{-6} for an HF radar.

4.5 Critical Viewing Geometry

Some echoes may not be fully formed because of the antenna's angular response. Wave diffraction and the associated phase behavior are responsible for the restrictive orthogonal geometry governing the radar's transverse reflection mode. There are two conditions necessary for a given meteor train to provide an echo: for the particular radar line-of-sight, the central Fresnel interval should be within the antenna's radiation pattern; and the scattered power should be above the detection threshold of the radar system. As discussed above, complete echoes can be expected in cases where a substantial fraction of the central Fresnel zone lies within the radiation pattern. This constraint is very strict, so that many meteors producing ionization trails above the observer's horizon within the antenna's beam but that are not formed with critically favorable geometry are undetectable. If the t_0 point is formed near the high elevation edge of the radar's beam, then contributions from pre-t_0 zones ($X < 0$) are attenuated, and the resulting echo is due dominantly to ionization situated with $X > 0$, and the large phase growth is absent. Conversely, meteor trains formed near the low elevation edge of the antenna's beam can only produce contributions from the $X < 0$ region. Radars employing very narrow (pencil-beam) antenna radiation patterns – so that the size of the Fresnel interval is comparable with the physical distance intercepted by the antenna at the echoing altitude – will sample a large proportion of such truncated echoes.

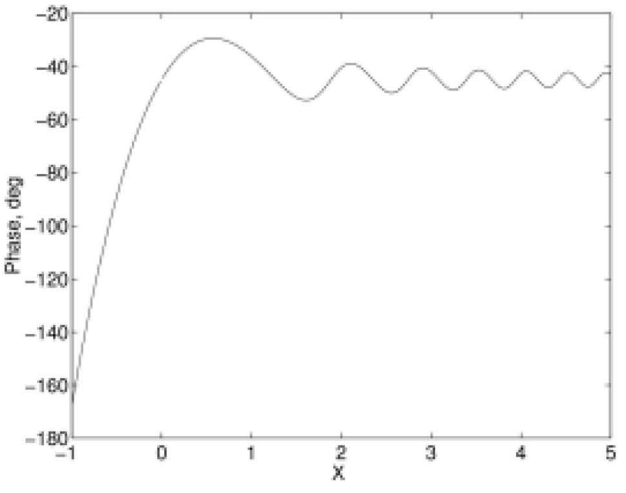

Figure 14. The phase (in degrees) of the scattered electric field for longitudinal polarization with X as the Fresnel parameter proportional to time. The phase was normalized to a value of $-45°$ at the t_0 point when $X = 0$.

4.6 Additional Factors

In order to complete the description of the interaction of radio waves with meteoric ionization trains and the characteristics of radar signatures, there are additional effects that need attention. Their impacts depend on sampling wavelength; the speed of the meteoroid; the state of the atmosphere; and the finite initial radius of the plasma, a value that depends on height and meteoroid velocity. The finite speed means that diffusion of the train results in a larger train radius at greater heights. The medium below the reflection height may impose Faraday rotation of the plane of polarization and absorption. These factors have been previously summarized [60].

5. Conclusions

It has been 80 years since the earliest radio reports of transient ionospheric echoes that were recognized in due course as meteors. Early investigators of the ionosphere sought to understand the fleeting phenomenon of nature that radio transmissions detected, while theoretical work was later able to formulate our understanding of the echo signatures. Radar meteors are now a valuable tool in many areas: atmospheric probing of density, temperature, and wind-field behavior (for example, [61]), in height regimes difficult to access by other means. They are a tool that opened up a whole new perspective of astronomical monitoring of objects impacting into the Earth's atmosphere and the solar system dust cloud. Radar techniques allowed us to measure the speed of meteoroids through the atmosphere and, using multiple sites, to determine their orbits in space [62, 63].

6. References

1. R. A. Heising, "Experiments and Observations Concerning the Ionized Regions of the Atmosphere," *Proc. Inst. Radio Engn.*, **16**, 1928, pp. 75-99.

2. T. L. Eckersley, "An Investigation of Short Waves," *J. Instn. Elec. Engrs.*, **67**, 1929, pp. 992-1028.

3. E. V. Appleton, "On Some Measurements of the Equivalent Height of the Atmospheric Ionized Layer," *Proc. Roy. Soc.*, **A126**, 1930, pp. 542-569.

4. A. M. Skellett, "The Effect of Meteors on Radio Transmission Through the Kennelly-Heavyside Layer," *Phys. Rev.*, **37**, 1931, p. 1668.

5. G. W. Pickard, "A Note on the Relation of Meteor Showers and Radio Reception," *Proc. Inst. Radio Engn.*, **19**, 1931, pp. 1166-1170.

6. E. V. Appleton and R. Naismith, "Some Measurements of Upper-Atmospheric Ionization," *Proc. Roy. Soc.*, **A137**, 1932, pp. 36-54.

7. J. P. Schafer and W. M. Goodall, "Kennelly-Heaviside Layer Studies Employing a Rapid Method of Virtual-Height Determination," *Proc. Inst. Radio Engn.*, **20**, 1932, pp. 1131-1148.

8. J. P. Schafer and W. M. Goodall, "Observations of Kennelly-Heaviside Layer Heights During the Leonid Meteor Shower of November 1931," *Proc. Inst. Radio Engn.*, **20**, 1932, pp. 1941-1945.

9. A. M. Skellett, "The Ionizing Effect of Meteors in Relation to Radio Propagation," *Proc. Inst. Radio Engn.*, **20**, 1932, pp. 1933-1939.

10. E. V. Appleton and R. Naismith, "Weekly Measurements of Upper-Atmospheric Ionization," *Proc. Phys. Soc.*, **45**, 1933, pp. 389-398.

11. J. A. Ratcliffe and E. L. C. White, "Some Automatic Records of Wireless Waves Reflected from the Ionosphere," *Proc Phys. Soc.*, **46**, 1934, pp. 107-115.

12. S. K. Mitra, P. Syam and B. N. Ghose, "Effect of a Meteoric Shower on the Ionosphere," *Nature*, **133**, 1934, pp. 533-534.

13. A. M. Skellett, "The Ionizing Effect of Meteors," *Proc. Inst. Radio Engn.*, **23**, 1935, pp. 132-149.

14. E. V. Appleton, R. Naismith and L. J. Ingram, "British Radio Observations During the Second International Polar Year 1932-33," *Phil. Trans.*, **A236**, 1937, pp. 191-259.

15. R. A. Watson Watt, A. F. Wilkins and E. G. Bowen, "The Return of Radio Waves from the Middle Atmosphere," *Proc. Roy. Soc.*, **A161**, 1937, pp. 181-196.

16. J. N. Bhar, "Effect of Meteoric Shower on the Ionization of the Upper Atmosphere," *Nature*, **139**, 1937, pp. 470-471.

17. T. L. Eckersley, "Irregular Ionic Clouds in the E-Layer of the Ionosphere," *Nature*, **140**, 1937, pp. 846-847.

18. A. M. Skellett, "Meteoric Ionization in the E Region of the Ionosphere," *Nature*, **141**, 1938, p. 472.

19. J. A. Pierce, "Abnormal Ionization in the E Region of the Ionosphere," *Proc. Inst. Radio Engn.*, **26**, 1938, pp. 892-908.

20. E. V. Appleton and J. H. Piddington, "The Reflexion Coefficients of Ionospheric Regions," *Proc. Roy. Soc.*, **A164**, 1938, pp. 467-476.

21. E. V. Appleton, R. Naismith, and L. T. Ingram, "The Critical-Frequency Method of Measuring Upper-Atmospheric Ionization," *Proc. Phys. Soc.*, **51**, 1939, pp. 81-92.

22. T. L. Eckersley, "Analysis of the effect of Scattering in Radio Transmission," *J. Instn. Elec. Engn.*, **86**, 1940, pp. 548-567.

23. P. M. S. Blackett and A. C. B. Lovell, "Radio Echoes and Cosmic Ray Showers," *Proc. R. Soc. London*, **177**, 1941, pp. 183-186.

24. C. D. Ellyett, private communication

25. J. A. Pierce, "A Note on Ionization by Meteors," *Phys. Rev.*, **59**, 1941, pp. 625-628.

26. T. L. Eckersley and F. T. Farmer, "Short Period Fluctuations in the Characteristics of Wireless Echoes from the Ionosphere," *Proc. Roy. Soc.*, **A184**, 1945, pp. 196-214.

27.E. V. Appleton, "The Scientific Principles of Radiolocation," *Instn. Elec. Engn.*, **92**, 1945, p. 340.

28.O. P. Ferrell, "Meteoric Impact Ionization Observed on Radar Oscilloscopes," *Phys. Rev.*, **69**, 1946, pp. 32-33.

29. J. S. Hey and G. S. Stewart, "Derivation of Meteor Stream Radiants by Radio Reflexion Methods," *Nature*, **158**, 1946, pp. 481-482.

30. J. S. Hey and G. S. Stewart, "Radar Observations of Meteors," *Proc. Phys. Soc., London*, **59**, 1947, pp. 858-883.

31.J. P. M. Prentice, A. C. B Lovell and C. J. Banwell, "Radio Observations of Meteors," *Mon. Not. Roy. Astr. Soc.*, **107**, 1947, pp. 155-163.

32.D. W. R. McKinley and P. M. Millman, "A Phenomenological Theory of Radar Echoes from Meteors," *Proc. Inst, Radio Engn.*, **37**, 1949, pp. 364-375.

33.E. V. Appleton and R. Naismith, "Radar Detection of Meteor Trails," *Nature*, **158**, 1946, pp. 936-938.

34.E. V. Appleton and R. Naismith, "The Radio Detection of Meteor Trails and Allied Phenomena," *Proc. Phys. Soc.*, **59**, 1947, pp. 461-473.

35.J. A. Pierce, "Ionization by Meteoric Bombardment," *Phys. Rev.*, **71**, 1947, pp. 88-92.

36.T. L. Eckersley, "Evaporation of Meteors," *Nature*, **160**, 1947, p. 91.

37.E. Eastwood and K. A. Mercer, "A Study of Transient Radar Echoes from the Ionosphere," *Proc. Phys., Soc.*, **61**, 1948, pp. 122-134.

38.E. W. Allen, "Reflections of Very-High-Frequency Radio Waves from Meteoric Ionization," *Proc. IRE*, **36**, 1948, pp. 346-353.

39.L. A. Manning and O. G. Villard, "VHF Reflections from Meteors," *Proc. IRE*, **36**, 1948, pp. 1255-1257.

40.A. C. B. Lovell and J. A. Clegg, "Characteristics of Radio Echoes from Meteor Trails: I. Intensity of the Radio Reflections and Electron Density in the Trails," *Proc. Phys. Soc. London*, **60**, 1948, pp. 491-498.

41.T. R. Kaiser and R. L. Closs, "Theory of Radio Reflections from Meteor Trails I," *Phil. Mag.*, **43**, 1952, pp. 1-32.

42. J. D. Mathews, D. D. Meisel, K. P. Hunter, V. S. Getman, Q. Zhou, "Very High Resolution Studies of Micrometeors Using the Arecibo 430 MHz Radar," *Icarus*, **126**, 1997, pp. 157-169.

43.A. Pellinen-Wannberg, G. Wannberg, J. Kero, C. Szasz and A. Westman. "The Impact of High-Resolution Radar on Meteor Studies: The EISCAT Perspective," *The Radio Science Bulletin*, No. 324, 2008, pp. 17-28.

44.E. M. Poulter and W. J. Baggaley, "Radiowave Scattering from Meteoric Ionization," *J. Atmos. Terr. Phys.*, **39**, 1977, pp. 757-764.

45. Y. Dimant and M. Oppenheim, "Meteor Trail Diffusion: 1. Simulations," *J. Geophys. Res.*, **111**, 2006, DOI:10.1029/2006JA011797.

46.D. W. R, McKinley, "Radar Echo Durations and Height of a Perseid Meteor," *J. Atmos. Terr. Phys.*, **8**, 1956, pp. 76-82.

47.W. J. Baggaley, "The De-Ionization of Dense Meteor Trains," *Planet. Space Sci.*, **26**, 1978, pp. 979-981.

48.W. J. Baggaley, "The Interpretation of Overdense Radio Meteor Echo Duration Characteristics," *Bull. Astr. Instit. Czech.*, **30**, 1979, p. 184.

49.J. Jones, B. A. McIntosh, and M. Simek, "Ozone and the Duration of Overdense Radio Meteors," *J. Atmos. Terr. Phys.*, **52**, 1990, pp. 253-258.

50.CIRA-86, in D. Rees (ed.), "COSPAR International Reference Atmosphere: 1986, Part I: Thermosphere Models," *Adv. Space Res.*, **8**, 5-6, 1988.

51.Y. Dimant and M. Oppenheim, "Meteor Trail Diffusion: 2. Analytical Theory," *J. Geophys. Res.*, **111**, 2006, DOI:10.1029/2006JA011798.

52.Q.-H. Zhou, J. D. Mathews and T. Nakamura, "Implications of Meteor Observations by the MU Radar," *Geophys. Res. Lett.*, **28**, 2001, pp. 1399-1402.

53.J. D. Mathews, "Radio Science Issues Surrounding HF/VHF/UHF Radar Meteor Studies," *J. Atmos. Sol. Terr. Phys.*, **66**, 2004, pp. 285-299.

54.A. Malhotra, J. D. Mathews and J. Urbina, "A Radio Science Perspective on Long-Duration Meteor Trails," *J. Geophys. Res.*, **112**, A12303, 2007, doi:10.1029/2007JA012576.

55.J. Jones and W. Jones, "Oblique Scattering of Radio Waves from Meteor Trains – Long Wavelength Approximation," *Planet. Space Sci.*, **38**, 1990, pp. 925-932.

56.C. D. Ellyett and J. G. Davies, "Velocity of Meteors Measured by Diffraction of Radio Waves from Trails During Formation," *Nature*, **161**, 1948, pp. 596-597.

57.W. J. Baggaley and J. Grant, "Techniques for Measuring Radar Meteor Speeds," *Earth Moon and Planets*, **95**, 2005, pp. 601-615.

58.W. K. Hocking, "Real-Time Meteor Entrance Speed Determinations Made with Interferometric Meteor Radars," *Radio Sci.*, **35**, 2000, pp. 1205-1220.

59.W. J. Baggaley, R. G. T. Bennett and A. D. Taylor, "Radar Meteor Atmospheric Speeds Determined from Echo Profile Measurements," *Planet. Space Sci.*, **45**, 1997, pp. 577-583.

60.Z. Ceplecha, J. Borovicka, W. G. Elford, D. O. ReVelle, R. L. Hawkes, V. Porubcan, and M. Šimek, "Meteor Phenomena and Bodies," *Space Sci. Rev.*, **84**, 1998, pp. 327-471.

61.Ch. Jacobi, K. Fröhlich, C. Viehweg, G. Stober, and D. Kürschner, "Midlatitude Mesosphere/Lower Thermosphere Meridional Winds and Temperatures Measured with Meteor Radar," *Advances in Space Research*, **39**, 8, 2007, pp. 1278-1283.

62.W. J. Baggaley, R. G. T. Bennett, D. I. Steel and A. D. Taylor, "The Advanced Meteor Orbit Radar: AMOR," *Q. J. Roy. Astron. Soc.*, **35**, 1994, pp. 293-320.

63.J. Jones, P. Brown, K. J. Ellis, A. R. Webster, M. Campbell-Brown, Z. Krzemenski and R. J. Weryk, "The Canadian Meteor Orbit Radar: System Overview and Preliminary Results," *Planet. Space Sci.*, **53**, 2005, pp. 413-421.